JOURNAL OF AGRICULTURAL AND FOOD CHEMISTRY

Characterization of Phenolic Compounds in Rooibos Tea

NICOLE KRAFCZYK AND MARCUS A. GLOMB*

Institute of Chemistry, Food Chemistry, Martin Luther University Halle-Wittenberg, Kurt-Mothes-Strasse 2, 06120 Halle, Germany

Polyphenols present in rooibos, a popular herbal tea from *Aspalathus linearis,* were isolated in two steps. First, phenolic ingredients were separated by multilayer countercurrent chromatography (MLCCC). Preparative high-performance liquid chromatography (HPLC) was then applied to obtain pure flavonoids. The purity and identity of isolated compounds was confirmed by different NMR experiments, HPLC-diode array detector (DAD), or gas chromatography−mass spectrometry (GC-MS) analysis. This strategy proved to be valid to isolate material in up to gram quantities and to verify known and previously not published polyphenol structures. In addition the chemistry of dihydrochalcones and related intermediates was studied. The dihydrochalcone aspalathin was oxidized to the corresponding flavanone-*C*-glycosides ((*R*)/(*S*)-eriodictyol-6-*C*-β-D-glucopyranoside and (*R*)/(*S*)-eriodictyol-8-*C*-β-D-glucopyranoside). Flavanone-6-*C*-β-D-glucopyranosides were further degraded to flavones isoorientin and orientin.

KEYWORDS: Rooibos tea; multilayer countercurrent chromatography (MLCCC); reactions of dihydrochalcones; NMR; HPLC-DAD; HR-(GC)-MS

INTRODUCTION

Rooibos is a shrubby legume that is indigenous to the mountains of South African's Western Cape. The genus *Aspalathus* includes more than 200 species native to South Africa, but only *Aspalathus linearis* (*A. linearis*) is edible (*1*). Its leaves and stems are used for the production of rooibos tea, a beverage with acclaimed beneficial health effects. Rooibos tea boasts high yields of flavonoids with exceptional high contents in *C*-glycosides. Furthermore, this tea is rich in minerals, is caffeine-free, and has low tannin contents (*2*). Usually, two types of rooibos are available, unfermented and fermented rooibos tea. The fermentation process is an oxidation process brought about for the formation of the characteristic red-brown color and sweetish flavor of the infusion.

First determination of phenolic ingredients of *A. linearis* was established by Koeppen et al. (*3–5*). The presence of aspalathin, orientin, isoorientin, isoquercitrin, and rutin was described after separation by paper chromatography. Other flavonoids like quercetin and luteolin have been isolated from processed rooibos tea by special extraction methods (*6*). Furthermore, vitexin, isovitexin, chrysoeriol, and some phenolic acids such as *p*-hydroxybenzoic acid, protocatechuic acid, caffeic acid, vanillic acid, *p*-coumaric acid, and ferulic acid were identified in processed rooibos (*7*). The occurrence of nothofagin, (*S*)- and (*R*)-eriodictyol-6-*C*-β-D-glucopyranoside, syringic acid, and (+)-catechin was established (*8, 9*). The content of the dihydrochalcones aspalathin and nothofagin, the major *C*-glycosylflavonoids in unfermented rooibos, decreased significantly with processing (*10*). Marais et al. reported on the degradation of aspalathin during fermentation to the flavanones (*S*)- and (*R*)-eriodictyol-6-*C*-β-D-glucopyranoside (*9*).

Separation and purification of rooibos using conventional methods such as column chromatography and high-performance liquid chromatography (HPLC) requires several steps resulting in low amounts of products. Multilayer countercurrent chromatography (MLCCC) is a unique liquid–liquid partition chromatography, which uses no solid matrix. Therefore, it eliminates irreversible adsorptive loss of samples onto the solid support used in conventional chromatographic setups. This method has been successfully applied to analysis and separation of various natural products (*11*). The aim of this work was to comprehensively isolate phenolic compounds from rooibos by MLCCC and preparative HPLC. In addition, the oxidative degradation mechanism of dihydrochalcones was studied in-depth.

MATERIALS AND METHODS

Chemicals. Chemicals of the highest quality available were obtained from Roth (Karlsruhe, Germany) unless otherwise indicated. Methanol was HPLC grade from Merck (Darmstadt, Germany). Caffeic acid, ferulic acid, heptafluorobutyric acid, *p*-hydroxybenzoic acid, (+)-catechin, and pyridine were purchased from Fluka (Taufkirchen, Germany). Dimethyl sulfoxide (DMSO-d_6) was obtained from Chemotrade (Leipzig, Germany). Gallic acid was ordered from Serva (Heidelberg, Germany). Vanillic acid, sinapinic acid, *p*-coumaric acid,

* To whom correspondence should be addressed. Fax: +49-345-5527341. E-mail: marcus.glomb@chemie.uni-halle.de.

10.1021/jf703701n CCC: $40.75
Published on Web 04/10/2008

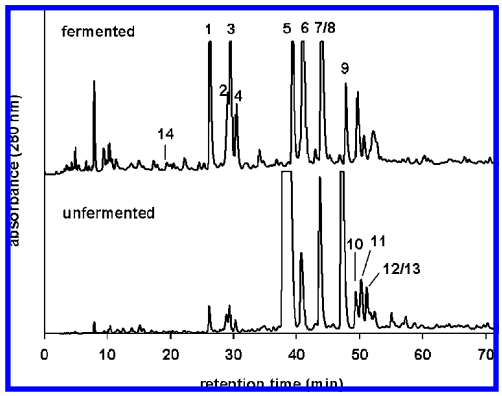

Figure 1. HPLC-DAD chromatogram of ethyl acetate extract from fermented and unfermented rooibos tea at $\lambda = 280$ nm. Retention times are given in parentheses: **1**, (*S*)-eriodictyol-6-*C*-β-D-glucopyranoside (26.3 min); **2**, (*S*)-eriodictyol-8-*C*-β-D-glucopyranoside (29.1 min); **3**, (*R*)-eriodictyol-6-*C*-β-D-glucopyranoside (29.5 min); **4**, (*R*)-eriodictyol-8-*C*-β-D-glucopyranoside (30.4 min); **5**, aspalathin (39.4 min); **6**, orientin (40.9 min); **7**/**8**, isoorientin/vitexin (44.1 min); **9**, nothofagin (47.8 min); **10**, isovitexin (49.7 min); **11**, rutin (50.6 min); **12**, hyperoside (51.6 min); **13**, isoquercitrin, (52.1 min) **14**, chlorogenic acid (19.3 min).

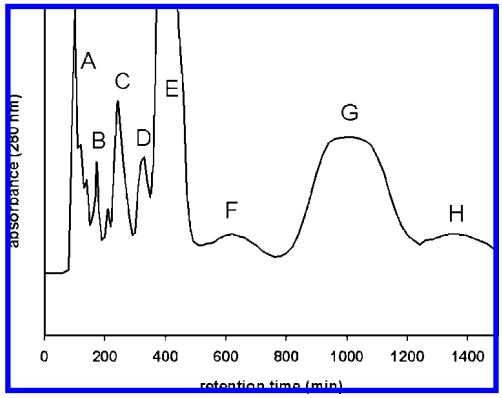

Figure 2. Separation of ethyl acetate extract from unfermented rooibos tea by MLCCC: A, mixture of flavonoids; B, (*S*)-eriodictyol-8-*C*-β-D-glycopyranoside (**2**); C, chlorogenic acid (**14**), (*S*)-eriodictyol-6-*C*-β-D-glucopyranoside (**1**), (*R*)-eriodictyol-6-*C*-β-D-glucopyranoside (**3**), (*R*)-eriodictyol-8-*C*-β-D-glucopyranoside (**4**), and rutin (**11**); D, isoorientin (**7**); E, aspalathin (**5**); F, orientin (**6**) and vitexin (**8**); G, nothofagin (**9**) and isovitexin (**10**); H, hyperoside (**12**) and isoquercitrin (**13**).

and *N*,*O*-bis(trimethylsilyl)acetamide were obtained from Sigma-Aldrich (Taufkirchen, Germany). Salicylic acid was ordered from Kosmos (Stuttgart, Germany).

Extraction of Rooibos Tea. Rooibos tea from the Biedouw Valley of South Africa was obtained from Ronnefeldt (Worpswede, Germany). A 100 g amount of fermented (red-brownish) or unfermented (green) rooibos was extracted with acetone/water (7:3 (v/v)) at 5 °C for 24 h under argon atmosphere and decanted. Acetone was removed under reduced pressure. The residual H_2O phase was successively extracted with diethyl ether (2 × 200 mL), ethyl acetate (2 × 200 mL), and *n*-butanol (2 × 200 mL). From the individual extracts, solvents were removed under reduced pressure.

Multilayer Countercurrent Chromatography. The MLCCC system (Ito, Multilayer Separator-Extractor Model, P.C. Inc., Potomac) was equipped with a Waters constant-flow pump (model 6000 A), a Zeiss spectraphotometer PM2D operating at 280 nm, and a sample injection valve with a 10 mL sample loop. Eluted liquids were collected in fractions of 8 mL with a fraction collector (LKB Ultrorac 7000). Chromatograms were recorded on a plotter (Servogor 200). The multilayer coil was prepared from 1.6 mm i.d. poly(tetrafluoraethylene) (PTFE) tubing. The total capacity was 300 mL. The MLCCC was run at a revolution speed of 800 rpm and a flow rate of 2 mL/min in head to tail modus.

Samples of 1 g were dissolved in a 1:1 mixture (10 mL) of light and heavy phase and injected into the system. The solvent system for separation of ethyl acetate extract or *n*-butanol extract consisted of ethyl acetate/*n*-butanol/water (3:1:4 (v/v)). Diethyl ether extracts were separated by using water/ethyl acetate (2:1 (v/v)).

Analytical HPLC-DAD. A Jasco (Gross-Umstadt, Germany) quaternary gradient unit PU 2080, with degasser DG 2080-54, autosampler AS 2055, column oven (Jasco Jetstream II), and multiwavelength detector MD 2015 was used. Chromatographic separations were performed on stainless steel columns (VYDAC CRT, no. 218TP54, 250 × 4.0 mm, RP 18, 5 μm, Hesperia, CA) using a flow rate of 1.0 mL min^{-1}. The mobile phase used was water (solvent A) and MeOH/water (7:3 (v/v), solvent B). To both solvents (A and B), 0.6 mL/L heptafluorobutyric acid (HFBA) was added. Samples were injected at 10% B; the gradient then changed linear to 30% B in 30 min, to 65% B in 40 min, and to 100% B in 2 min and were held at 100% B for 8 min. The column temperature was 25 °C. The effluent was monitored at 280 and 350 nm.

Preparative HPLC-UV. A Besta HD 2-200 pump (Wilhelmsfeld, Germany) was used at a flow rate of 8 mL min^{-1}. Elution of materials was monitored by a UV detector (Jasco UV- 2075, Gross-Umstadt). Chromatographic separations were performed on stainless steel columns (VYDAC CRT, no. 218TP1022, 250 × 23 mm, RP18, 10 μm, Hesperia, CA). The mobile phase used was solvents A and B, identical to the analytical HPLC-DAD system. From the individual chromatographic fractions, solvents were removed under reduced pressure. After addition of water, solutions of polyphenols were freeze-dried.

Preparative Thin-Layer Chromatography (TLC). Separation was performed on silica gel 60 F_{254} plates, 2 mm (Merck), with ethyl acetate/hexane (1:1 (v/v)) as the mobile phase. For isolation of substances, spots were scratched off. Then, target material was eluted from silica gel with methanol.

Accurate Mass Determination. The high-resolution positive and negative ion ESI mass spectra (HR-MS) were obtained from a Bruker Apex III Fourier transform ion cyclotron resonance (FT-ICR) mass spectrometer (Bruker Daltonics, Billerica, USA) equipped with an Infinity cell, a 7.0 T superconducting magnet (Bruker, Karlsruhe, Germany), a radio frequency (RF)-only hexapole ion guide and an external electrospray ion source (APOLLO; Agilent, off-axis spray). Nitrogen was used as the drying gas at 150 °C. The samples were dissolved in methanol, and the solutions were introduced continuously via a syringe pump at a flow rate of 120 μL h^{-1}. The data were acquired with 256*k* data points and zero filled to 1024*k* by averaging 32 scans.

Magnetic Resonance Spectroscopy. Nuclear magnetic resonance (NMR) spectra were recorded on a Varian Unity Inova 500 instrument (Darmstadt, Germany). Chemical shifts are given relative to external Me_4Si.

*NMR Data of Vitexin (**8**).* ^{1}H NMR (DMSO-d_6): δ 6.76 (1 H, s, H3), 6.26 (1 H, s, H6), 8.01 (2 H, d, $J = 8.7$ Hz, H2′, H6′), 6.87 (2 H, d, $J = 8.7$ Hz, H3′, H5′), 4.67 (1 H, d, $J = 9.8$ Hz, H1″), 3.81 (1 H, t, $J = 9.7$ Hz, H2″), 3.29 (1 H, m, H3″), 3.37 (1 H, t, $J = 9.2$ Hz, H4″), 3.23 (1 H, m, H5″), 3.75 (1 H, dd, $J = 11.9$ Hz, 2.2 Hz, H6a″), 3.51 (1 H, dd, $J = 6.0$ Hz, 11.7 Hz, H6b″) ppm. ^{13}C NMR (DMSO-d_6): δ 163.91 (C2), 102.41 (C3), 182.06 (C4), 155.96 (C5), 98.10 (C6), 162.51 (C7), 104.01 (C8), 160.35 (C9), 104.58 (C10), 121.57 (C1′), 128.92 (C2′, C6′), 115.77 (C3′, C5′), 161.10 (C4′), 73.34 (C1″), 70.80 (C2″), 78.63 (C3″), 70.51 (C4″), 81.81 (C5″), 61.26 (C6″) ppm.

*NMR Data of Isovitexin (**10**).* ^{1}H NMR (DMSO-d_6): δ 6.77 (1 H, s, H3), 6.51 (1 H, s, H 8), 7.91 (2 H, d, $J = 8.8$ Hz, H2′, H6′), 6.91 (2 H, d, $J = 8.8$ Hz, H3′, H5′), 4.57 (1 H, d, $J = 9.9$ Hz, H1″), 4.02 (1 H, t, $J = 8.9$ Hz, H2″), 3.19 (1 H, t, $J = 8.5$ Hz, H3″), 3.11 (1 H, t, $J = 9.2$ Hz, H4″), 3.15 (1 H, m, H5″), 3.68 (1 H, dd, $J = 10.4$ Hz, H6a″), 3.40 (1 H, dd, $J = 5.9$ Hz, 10.4 Hz, H6b″) ppm. ^{13}C NMR (DMSO-d_6): δ 163.96 (C2), 103.22 (C3), 182.39 (C4), 161.60 (C5), 109.31 (C6), 163.67 (C7), 94.20 (C8), 156.64 (C9), 103.85 (C10),

Table 1. ^{1}H (500 MHz) and ^{13}C NMR (125 MHz) Spectroscopic Data of Dihydrochalcones Aspalathin (**5**) and Nothofagin (**9**) (in DMSO-d_6)[a]

	aspalathin		nothofagin	
	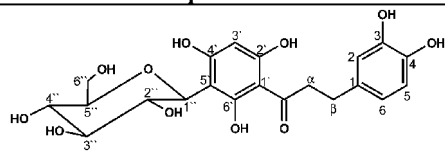		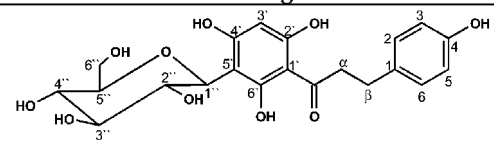	
C/H	δ^{1}H [ppm]	δ^{13}C [ppm]	δ^{1}H [ppm]	δ^{13}C [ppm]
1		132.35		131.58
2	6.60 (s, 1H)	115.69	7.00 (d, 2H, J = 8.5 Hz)	129.11
3		144.96	6.63 (d, 2H, J = 8.5 Hz)	115.03
4		143.23		155.35
5	6.60 (d, 1H, J = 10.8 Hz)	115.43	6.63 (d, 2H, J = 8.5 Hz)	115.03
6	6.46 (d, 1H, J = 6.0 Hz)	118.82	7.00 (d, 2H, J = 8.5 Hz)	129.11
α	3.20 (t, 2H, J = 8.2 Hz)	45.45	3.20 (t, 2H, J = 8.2 Hz)	45.55
β	2.70 (t, 2H, J = 7.5 Hz)	29.67	2.74 (t, 2H, J = 7.5 Hz)	29.53
1`		104.02		104.02
2`		161.59		161.58
3`	5.93 (s, 1H)	94.55	5,91 (s, 1H)	94.54
4`		164.75		164.73
5`		103.58		103.57
6`		164.61		163.62
1``	4.50 (d, 1H, J = 9.9 Hz)	73.54	4.49 (d, 1H, J = 9.7 Hz)	73.54
2``	3.86 (pt, 1H, J = 8.6 Hz)	70.43	3.85 (pt, 1H, J = 8.3 Hz)	70.41
3``	3.18 (pt, 1H, J = 8.2 Hz)	78.86	3.20 (pt, 1H, J = 8.3 Hz)	78.88
4``	3.09 (pt, 1H, J = 9.2 Hz)	70.63	3.12 (pt, 1H, J = 8.8 Hz)	70.64
5``	3.15 (m, 1H)	81.29	3.14 (m, 1H)	81.28
6``	3.40 (dd, 1H, J = 11.5 Hz, 6.4 Hz)	61.26	3.39 (dd, 1H, J = 11.5, 6.6 Hz)	61.25
	3.64 (dd, 1H, J = 11.3 Hz, 1.4 Hz)		3.62 (dd, 1H, J = 11.6, 2.2 Hz)	

[a] δ, chemical shift; J, coupling constant. Hydrogen/carbon assignments were verified by HMBC, HMQC, and ^{13}C-DEPT measurements.

121.53 (C1′), 128.90 (C2′, C6′), 116.41 (C3′, C5′), 161.08 (C4′), 73.48 (C1″), 70.64 (C2″), 79.37 (C3″), 71.04 (C4″), 82.00 (C5″), 61.57 (C6″) ppm.

Gas Chromatography. High-resolution GC-MS (HRGC-MS) was performed on a Finnigan Trace GC Ultra (Thermo Finnigan, Bremen, Germany): quartz capillary column (30 m, 0.32 I.D., HP-5, 0.25 μm; J&W Scientific, Cologne, Germany); injection port, 220 °C; He, 27.5 cm/s; split ratio, 1:10; detector, 270 °C. After injection of samples at 100 °C, the oven temperature was raised at 5 °C min^{-1} to 200 °C, then raised at 10 °C min^{-1} to 270 °C, and held for 25 min (temperature program 1). For temperature program 2 samples were injected at 200 °C, the oven temperature was then raised at 2.3 °C min^{-1} to 270 °C and held for 30 min. The gas chromatograph was connected to a Trace DSQ (Thermo Finnigan, Bremen, Germany): transfer line, 220 °C; EI at 70 eV; full scan, 50–650 *m/z*.

Derivatization of Samples. Isolated material from MLCCC separation of diethyl ether extracts was dissolved in 100 μL of pyridine, and 100 μL of *N,O*-bis(trimethylsilyl)acetamide was added. After a reaction time of 1 h at room temperature, the solution was injected into the GC-MS system.

Incubations. Isolated substances (4.5 mM) were dissolved in phosphate buffer (0.2 M, pH = 7.4) and incubated (37 °C) for 48 h in a shaker incubator (New Brunswick Scientific, New Jersey). After evaporation, the final residue was separated by HPLC-DAD.

RESULTS AND DISCUSSION

Isolation and Elucidation of Polyphenolic Ingredients. *Ethyl Acetate and n-Butanol Extracts.* Ethyl acetate and *n*-butanol extract were screened for polyphenols by analytical HPLC-DAD. Basically both extracts revealed the same ingredients. The HPLC-DAD chromatogram of ethyl acetate extract is shown in **Figure 1**. The first step of purification was separation of these extracts by MLCCC (**Figure 2**) into eight fractions (A−H). Stationary-phase retention was between 50 and 55%. Afterward, fractions A−H were separated by preparative HPLC to isolate pure substances. Final structural evidence was achieved by ^{1}H and ^{13}C NMR, as well as heteronuclear multiple quantum coherence (HMQC) and heteronuclear multiple bond correlation (HMBC) NMR experiments. In most cases, only very rudimentary previous NMR data of rooibos ingredients has been published . Therefore, it was necessary to reinvestigate some structures, present in *A. linearis.*

Two dihydrochalcone structures, aspalathin (**5**) and nothofagin (**9**), were isolated and identified from MLCCC peak E and G. NMR data of both substances are demonstrated in **Table 1**. The presence of the dihydrochalcone skeleton was evident from ^{13}C NMR (δ 45.45 ppm (C-α), 29.67 ppm (C-β), the HMBC correlation from H-β to C-1 (δ 132.35 ppm)) and from H-α to C-1′. HR-MS verified a molecular mass of *m/z* 452.1 for **5** (*m/z* 451.1248 (found); *m/z* 451.1246 (calculated for $C_{21}H_{23}O_{11}$) [M − H]$^-$) and a molecular mass of *m/z* 436.1 for **9** (*m/z* 435.1295 (found); *m/z* 435.1297 (calculated for $C_{21}H_{23}O_{10}$) [M − H]$^-$). In both dihydrochalcones glucose is fixed in the β-glycoside position, because the H-atom at position 1″ had a chemical shift of 4.50 ppm coupling to H 2$^-$ at ^{3}J = 9.8 Hz. ^{1}H NMR data from **5** were in line with Koeppen and Roux (*5, 12*) and Rabe et al. (*7*). Results from **9** were corresponding to Bramati et al. (*13*) and Hillis and Inoue (*14*).

Flavone-*C*-glycosides were isolated from MLCCC peak D (isoorientin (**7**)), peak F (orientin (**6**), vitexin (**8**)), and peak G (isovitexin (**10**)). NMR data of the flavone-8-*C*-β-D-glucopyranoside orientin and flavone-6-*C*-β-D-glucopyranoside isoorientin are specified in **Table 2**. In both structures glucose is bound in the β-glycoside position (δ ^{1}H = 4.66 ppm,^{3}J = 10.0 Hz and δ ^{1}H = 4.58 ppm, ^{3}J = 9.8 Hz, respectively). HR-MS delivered a molecular mass of *m/z* 448.1 for **6** (*m/z* 447.0930 (found); *m/z* 447.0933 (calculated for $C_{21}H_{19}O_{11}$) [M − H]$^-$) and a molecular mass of *m/z* 448.1 for **7** (*m/z* 447.0929 (found); *m/z* 447.0933 (calculated for $C_{21}H_{19}O_{11}$) [M − H]$^-$). The ^{1}H NMR data of flavone-*C*-glycosides were in line with Koeppen (*4*) and Rabe et al. (*7*).

The NMR data and HR-MS data verified the structure of **8**and **10**. These are isomers of **6** and **7** lacking the hydroxyl group at position 3′ (**Table 2**, R = H, orientin → vitexin, isoorientin → isovitexin). Therefore, 3′ and 5′ like 2′ and 6′ have the same chemical shift in ^{1}H and ^{13}C NMR experiments.

Table 2. ^{1}H (500 MHz) and ^{13}C NMR (125 MHz) Spectroscopic Data of Flavone-*C*-glycosides Orientin (**6**) and Isoorientin (**7**) (in DMSO-d_6)[a]

	flavone-8-*C*-*β*-D-glucopyranoside, orientin, R = OH		flavone-6-*C*-*β*-D-glucopyranoside, isoorientin, R = OH	
	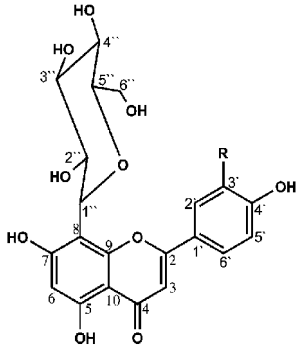		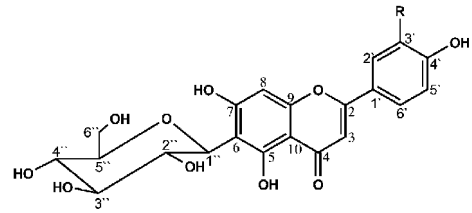	
C/H	δ ^{1}H [ppm]	δ ^{13}C [ppm]	δ ^{1}H [ppm]	δ ^{13}C [ppm]
2		164.05		163,63
3	6.63 (s, 1H)	102.36	6.66 (s, 1H)	102.79
4		181.98		181.86
5		162.50		160.67
6	6.26 (s, 1H)	98.06		108.85
7		160.34		163.22
8		104.51	6.47 (s, 1H)	93.48
9		156.95		156.18
10		103.99		103.40
1`		122.98		121.42
2`	7.41 (d, 1H, J = 7.6 Hz)	114.04	7.40 (d, 1H, J = 4.6)	113.30
3`		145.77		145.73
4`		149.77		149.68
5`	6.85 (d, 1H, J = 8.4 Hz)	115.61	6.88 (d, 1H, J = 8.4 Hz)	116.04
6`	7.52 (dd, 1H, ^{3}J = 6.2 Hz, ^{4}J = 2.2)	119.32	7.41 (dd, 1H, ^{3}J = 8.2 Hz, ^{4}J = 2.2)	118.96
1``	4.66 (d, 0.9H, J = 10.0 Hz) 4.82 (d, 0.1H, J = 9.2 Hz) *	73.35	4,57 (d, 1H, J = 9.8 Hz)	73.03
2``	3.84 (pt, 1H, J = 8.9 Hz)	70.73	4.02 (pt, 1H, J = 9.5 Hz)	70.60
3``	3.24 (pt, 1H, J = 8.9 Hz)	78.73	3.19 (pt, 1H, J = 8.7 Hz)	78.93
4``	3.36 (pt, 1H, J = 9.2 Hz)	70.66	3.13 (pt, 1H, J = 8.4 Hz)	70.19
5``	3.24 (m, 1H)	81.96	3.26 (m, 1H)	81.55
6``	3.68 (dd, 1H, J = 11.4 Hz, J = 1.2 Hz) 3.52 (dd, 1H, J = 11.7 Hz, J = 6.3 Hz)	61.60	3.67 (dd, 1H, J = 10.0 Hz, J = 2.1 Hz) 3.40 (dd, 1H, J = 10.0 Hz; J = 6.3 Hz)	61.48

[a] δ, chemical shift; J, coupling constant. Hydrogen/carbon assignments were verified by HMBC, HMQC, and ^{13}C-DEPT measurements. The asterisk (*) indicates rotamers (*21, 22*).

In both flavones the glucose was fixed in the β-glycoside position, too. HR-MS data from **8** delivered a molecular mass of *m/z* 432.1 (*m/z* 431.0986 (found); *m/z* 431.0984 (calculated for $C_{21}H_{19}O_{10}$) $[M - H]^-$) and a molecular mass of *m/z* 432.1 for **10** (*m/z* 431.0983 (found); *m/z* 431.0984 (calculated for $C_{21}H_{19}O_{10}$) $[M - H]^-$). UV and MS data of vitexin and isovitexin were corresponding to Rabe et al. (*7*) and Bramati et al. (*13*).

Four flavanone-*C*-glycosides (**1–4**) were isolated from MLCCC peaks B and C (**Figure 2**). **2** + **4** and **1** + **3** are diastereoisomeres, respectively, and gave different retention times in HPLC analysis. Although the absolute stereochemistry was not determined, the peak eluting first was tentatively assigned the S-isomer on the basis of Philbin and Schwartz (*15*). However, NMR results for each group were basically identical (**Table 3**). This must be due to the almost planar A and C ring system of the flavanone isomers resulting in an almost identical electronic environment for H-3 and H-2. Additionally, both pairs of diastereoisomeres are in equilibrium via ring opening to a quinine methide configuration. Incubations of isolated **1** in phosphate buffer resulted in immediate conversion to a 1:1 mixture of **1** + **3** (**Figure 3**). The NMR results are in line with the data from a diastereomeric mixture of (*R*)- and (*S*)-eriodictyol-6-*C*-*β*-D-glucopyranoside by Marais et al. (*9*). The data for the 8-*C*-glycosides are presented for the first time herein. HR-MS delivered a molecular mass of *m/z* 450.1 for **1** (*m/z* 449.10870 (found); *m/z* 449.1089 (calculated for $C_{21}H_{21}O_{11}$) $[M - H]^-$) and a molecular mass of *m/z* 449.1092 for **3** (*m/z* 449.1092 (found); *m/z* 449.1089 (calculated for $C_{21}H_{21}O_{11}$) $[M - H]^-$). Compound **2** gave a molecular mass of *m/z* 450.1 in HR-MS (*m/z* 449.1083 (found); *m/z* 449.1089 (calculated for $C_{21}H_{21}O_{11}$) $[M - H]^-$) and **4** gave a molecular mass of *m/z* 450.1 in HR-MS (*m/z* 449.1090 (found); *m/z* 449.1089 (calculated for $C_{21}H_{21}O_{11}$) $[M - H]^-$).

Flavonol-*O*-glycosides were isolated from MLCCC peak C (rutin **11**) and peak H (hyperoside (**12**) and isoquercitrin (**13**)). NMR data of these substances are shown in **Table 4**. The sugar of these three flavonol-*O*-glycosides is fixed in the β-glycoside position. Compound **11** gave the molecular mass *m/z* 610.1 (*m/z* 609.1465 (found); *m/z* 609.1461 (calculated for $C_{27}H_{29}O_{16}$) $[M - H]^-$), HR-MS delivered a molecular mass *m/z* 464.1 for **12** (*m/z* 503.0587 (found); *m/z* 503.0586 (calculated for $C_{21}H_{20}O_{12}K$) $[M + K]^+$), and a molecular mass *m/z* 464.1 for **13** (*m/z* 487.0859 (found); *m/z* 487.0847 (calculated for $C_{21}H_{20}O_{12}Na$) $[M + Na]^+$). All data for rutin were in line with Sawabe et al. (*16*).

Hyperoside was isolated from *A. linearis*, and the NMR data unequivocally were established for the first time in comparison to **13** and **11**. The detailed structure and selected HMBC correlations are shown in **Figure 4**. The presence of the flavone skeleton was evident from the UV (λ_{max} = 256 and 350 nm), ^{13}C NMR (δ 177 (C-4), 156 (C-2), and 133 ppm (C-3)), and

Table 3. ^{1}H and ^{13}C NMR Spectroscopic Data of Flavanone-*C*-glycosides (*R*)/(*S*)-Eriodictyol-6-*C*-*β*-D-glucopyranoside (**1** + **3**) and (*R*)/(*S*)-Eriodictyol-8-*C*-*β*-D-glucopyranoside (**2** + **4**) (in DMSO-d_6)[a]

	(*R*)/(*S*)-eriodictyol-8-*C*-*β*-D-glucopyranoside		(*R*)/(*S*)-eriodictyol-6-*C*-*β*-D-glucopyranoside	
	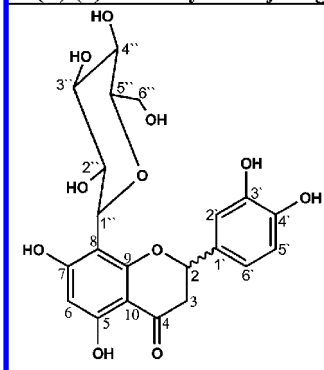		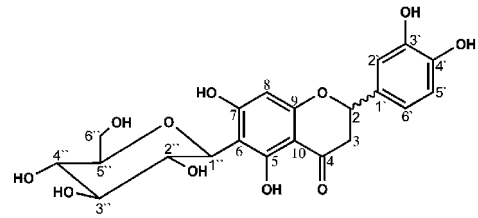	
	δ^{1}H [ppm]	δ^{13}C [ppm]	δ^{1}H [ppm]	δ^{13}C [ppm]
2	5.34 (dd, 1H, *J* = 2.9 Hz, 9.0 Hz)	78.65	5.34 (dd, 1H, *J* = 3.1 Hz, 9.0 Hz)	78.26
3_{cis}	2.70 (dd, 1H, *J* = 2.9 Hz, 14.2 Hz)	42.45	2.70 (dd, 1H, *J* = 3.1 Hz, 14.0 Hz)	42.05
3_{trans}	3.15 (dd, 1H, *J* = 9.0 Hz, 14.2 Hz)		3.15 (m, 1H)	
4		196.89		196.45
5		166.19		162.68
6	5.93 (s, 1H)	94.90		105.75
7		163.12		165.72
8		106.22	5.92 (s, 1H)	94.70
9		162.01		161.58
10		101.98		101.52
1`		129.87		129.41
2`	6.73 (s, 1H)	115.76	6.73 (s, 1H)	115.32
3`		145.64		145.18
4`		146.13		146.66
5`	6.86 (d, 1H, *J* = 10.6 Hz)	114.71	6.86 (d, 1H, *J* = 9.9 Hz)	114.24
6`	6.80 (d, 1H, *J* = 9.3 Hz)	118.30	6.75 (d, 1H, *J* = 7.5 Hz)	117.84
1``	4.46 (d, 1H, *J* = 9.8 Hz)	73.35	4.46 (d, 1H, *J* = 9.9 Hz)	72.93
2``	3.84 (pt, 1H, *J* = 9.8 Hz)	70.67	3.95 (pt, 1H, *J* = 9.1 Hz)	70.27
3``	3.16 (m, 1H)	79.49	3.15 (m, 1H)	79.03
4``	3.16 (m, 1H)	71.08	3.15 (m, 1H)	70.62
5``	3.16 (m, 1H)	81.93	3.15 (m, 1H)	81.47
6``	3.37 (dd, 1H, *J* = 5.7 Hz, 11.8 Hz)	61.96	3.38 (dd, 1H, *J* = 5.9 Hz, 11.9 Hz)	61.50
	3.65 (dd, 1H, *J* = 1.8 Hz, 11.8 Hz)		3.65 (dd, 1H, *J* = 1.8 Hz, 11.8 Hz)	

[a] *δ*, chemical shift; *J*, coupling constant. Hydrogen/carbon assignments were verified by HMBC, HMQC, and ^{13}C-DEPT measurements.

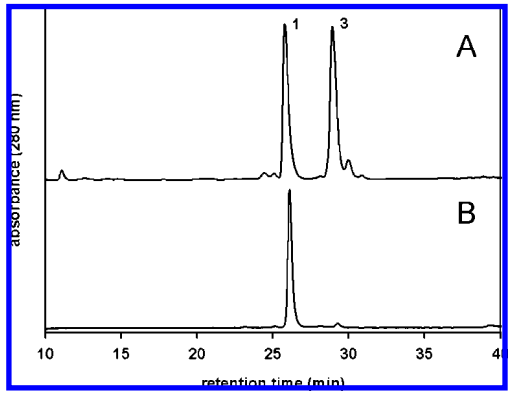

Figure 3. HPLC-DAD chromatogram of the incubation of **1** in phosphate buffer: (**A**) 24 and (**B**) 0 h.

the HMBC correlation from H-6 (*δ* 6.18 ppm, d, 1H, ^{4}J = 2 Hz) to C-5, C-7, C-8, and C-10. H-8 correlated to C-9, C-7, C-10, and C-6. The ^{1}H NMR spectrum displayed the anticipated systems for the A and B ring, the protons for 7-OH, 3′-OH, and 4′-OH (*δ* 9.1–12.6 ppm) and the chelated proton at 5-OH. The *β*-glycoside configuration was verified by H-1″ at *δ* 5.35 ppm coupling with ^{3}J = 7.7 Hz, which correlated to C-3 at 133.46 ppm. NMR data of **12** and **13** were identical to work published by Krasnov et al. (*17*).

From MLCCC peak B chlorogenic acid (5-*O*-caffeoyl-quinic acid (**14**)) was identified by comparing the retention time (RT = 19.3 min) and absorption spectrum (λ_{max} = 320 nm) to commercial reference material (**Figure 5**). Additionally, HR-MS gave a pseudo-molecular mass *m*/*z* 353.1 for **14** (*m*/*z* 353.0873 (found); *m*/*z* 353.0878 (calculated for $C_{16}H_{17}O_9$) [M − H]$^-$).

Diethyl Ether Extract. The diethyl ether extract was screened for polyphenols by analytical HPLC-DAD (**Figure 6**). In contrast to ethyl acetate and *n*-butanol extracts benzoic and cinnamic acids were found in high yields. In addition diethyl ether extract contained hydrophobic flavonoide aglycons. The extract was separated into eight signals (I−P) by MLCCC (**Figure 7**). Stationary-phase retention was between 60 and 65%. After workup, material was derivatized and subjected to coupled gas chromatography−mass spectrometry (temperature program 1). From the various MLCCC fractions the following polyphenolic structures were unequivocally identified by comparison with authentic material: syringic acid (**23**; *m*/*z*), 342 ($M^{+\bullet}$, 2× silylated, 62%), 327 (70%), 312 (64%), 297 (27%), 283 (25%), 253 (28%), 223 (25%), 141 (19%), 89 (9%), and 73 (100%); gallic acid (**15**; *m*/*z*), 458 ($M^{+\bullet}$, 4× silylated, 35%), 443 (16%), 281 (71%), 179 (11%), and 73 (100%); gentisic acid (**18**; *m*/*z*), 355 (M^{+} − 15, 3× silylated, 50%), 193 (10%), 147 (9%), and 73 (100%); protocatechuic acid (**16**; *m*/*z*), 370 ($M^{+\bullet}$, 2× silylated, 32%), 355 (18%), 311 (9%), 223 (5%), 193 (100%), 165 (8%), 137 (5%), and 73 (53%); vanillic acid (**21**; *m*/*z*), 312 ($M^{+\bullet}$, 2× silylated, 67%), 297 (100%), 282 (26%), 267 (69%), 253 (55%), 223 (29%), 193 (24%), and 73 (90%); caffeic acid

Table 4. ^{1}H and ^{13}C NMR Spectroscopic Data of Flavonol-*O*-glycosides Rutin (**11**), Hyperoside (**12**), and Isoquercitrin (**13**) (in DMSO-d_6)[a]

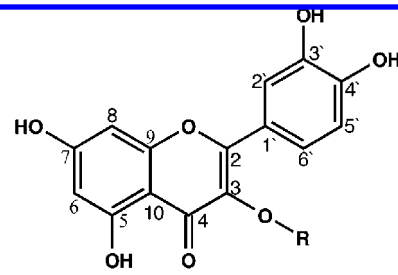

	isoquercitrin R = β-D-Glc		hyperoside R = β-D-Gal		rutin R = α-L-Rha-1→6-β-D-Glc	
	δ ^{1}H [ppm]	δ ^{13}C [ppm]	δ ^{1}H [ppm]	δ ^{13}C [ppm]	δ ^{1}H [ppm]	δ ^{13}C [ppm]
2		156.60		156.20		156.77
3		133.75		133.46		133.93
4		177.88		177.46		177.84
5		161.68		161.20		161.64
6	6.19 (d, 1H, J = 2.1 Hz)	99.07	6.18 (d, 1H, J = 2.0 Hz)	98.63	6.19 (d, 1H, J = 2.0 Hz)	99.11
7		164.53		164.09		164.54
8	6.39 (d, 1H, J = 2.0 Hz)	93.91	6.38 (d, 1H, J = 2.1 Hz)	93.46	6.39 (d, 1H, J = 2.0 Hz)	93.96
9		156.75		156.27		156.85
10		104.41		103.89		104.34
1`		121.60		121.07		121.50
2`	7.56 (d, 1H, J = 2.2 Hz)	116.63	7.50 (d, 1H, J = 2.3 Hz)	115.91	7.51 (d, 1H, J = 2.3 Hz)	116.42
3`		145.23		144.80		145.24
4`		148.88		148.43		148.91
5`	6.83 (d, 1H, J = 9.0 Hz)	115.63	6.79 (d, 1H, J = 8.5 Hz)	115.15	6.81 (d, 1H, J = 8.5 Hz)	115.61
6`	7.57 (dd, 1H, J = 2.2 Hz, 6.8 Hz)	122.02	7.64 (dd, 1H, J = 2.2 Hz, 8.5 Hz)	121.97	7.64 (dd, 1H, J = 2.3 Hz, 8.5 Hz)	122.35
1``	5.45 (d, 1H, J = 7.4 Hz)	101.30	5.35 (d, 1H, J = 7.7 Hz)	101.77	5.31 (d, 1H, J = 7.7 Hz)	102.44
2``	3.23 (m, 2H)	74.52	3.55 (dd, 1H, J = 9.4 Hz, 7.7 Hz)	75.81	3.04-3.31 (m, 8H)	74.50
3``	3.23 (m, 2H)	76.94	3.35 (m, 1H)	73.16		76.87
4``	3.07 (m, 2H)	70.37	3.63 (d, 1H, J = 3.2 Hz)	67.89		70.86
5``	3.07 (m, 2H)	78.00	3.29 (dd, 1H, J = 6.1 Hz, 5.9 Hz)	71.17		76.34
6a``	3.30 (m)	61.41	3.35 (m)	60.10	3.35 (dd, 1H, J = 6.1 Hz, 12.3 Hz)	67.41
6b``	3.57 (dd, 1H, J = 3.5 Hz, 11.5 Hz)		3.43 (dd, 1H, J = 5.5 Hz, 10.0 Hz)		3.69 (dd, 1H, J = 3.2 Hz, 10.0 Hz)	
1```					4.40 (dd, 1H, J =15.6 Hz, 1.3 Hz)	101.2
2```					3.04-3.31 (m, 8H)	70.79
3```						70.43
4```						72.27
5```						68.47
6```					1.03 (d, 3H, J = 6.2 Hz)	18.34

[a] δ, chemical shift; J, coupling constant. Hydrogen/carbon assignments were verified by HMBC, HMQC, and ^{13}C-DEPT measurements.

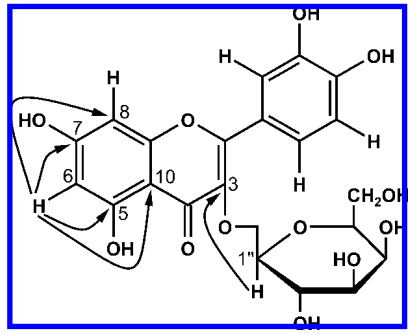

Figure 4. Structure of hyperoside **12**. Selected HMBC correlations are marked by arrows.

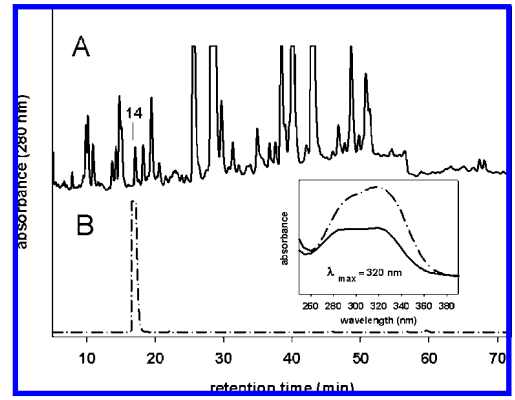

Figure 5. HPLC-DAD chromatograms of *n*-butanol extract (**A**) and chlorogenic acid (**B**). Both gave a peak at 19.3 min with identical absorption spectra, λ = 320 nm.

(**22**; *m/z*), 396 ($M^{+\bullet}$, 3× silylated, 17%), 219 (16%), 207 (11%), 147 (21%), and 75 (100%). As an example the identification of **23** is shown in **Figure 8**. Results from protocatechuic acid, caffeic acid, and vanillic acid were corresponding to Lin and Harnly (*18*). Data from **23** were in line with Ferreira et al. (*8*).

After MLCCC separation the retarded stationary phase was also silylated and separated by HRGC-MS (temperature program 1), leading to the identification of the following structures: 3,5-dihydroxybenzoic acid (**16**; RT = 18.3 min) *m/z* 370 ($M^{+\bullet}$, 3× silylated, 35%), 355 (10%), 281 (6%), 193 (100%), 147 (16%), and 73 (84%); *p*-hydroxybenzoic acid (**19**; RT = 14.2 min), *m/z* 282 ($M^{+\bullet}$, 2× silylated, 12%), 267 (86%), 223 (78%), 193 (41%), 147 (29%), and 75 (100%); *p*-coumaric acid (**24**; RT >

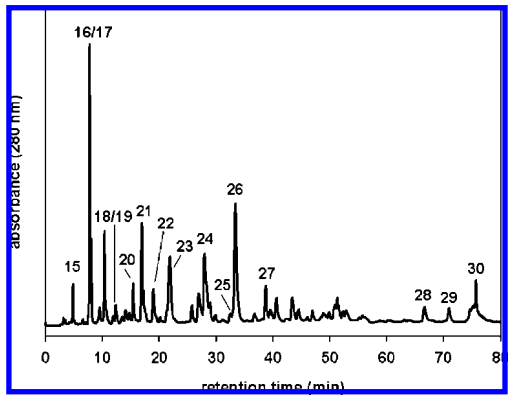

Figure 6. HPLC-DAD chromatogram of diethyl ether extract from unfermented rooibos tea at $\lambda = 280$ nm. Retention times are given in parentheses: **15**, gallic acid (4.9 min); **16**, protocatechuic acid (7.8 min); **17**, 3,5-dihydroxybenzoic acid (7.8 min); **18**, gentisic acid (12.3 min); **19**, *p*-hydroxybenzoic acid (12.3 min); **20**, (+)-catechin (15.9 min); **21**, vanillic acid (17.0 min); **22**, caffeic acid (19.0 min); **23**, syringic acid (21.9 min); **24**, *p*-coumaric acid (28.0 min); **25**, salicylic acid (32.7 min); **26**, ferulic acid (33.4 min); **27**, sinapinic acid (38.7 min); **28**, quercetin (66.7 min); **29**, luteolin (70.9 min); **30**, chrysoeriol (75.7 min).

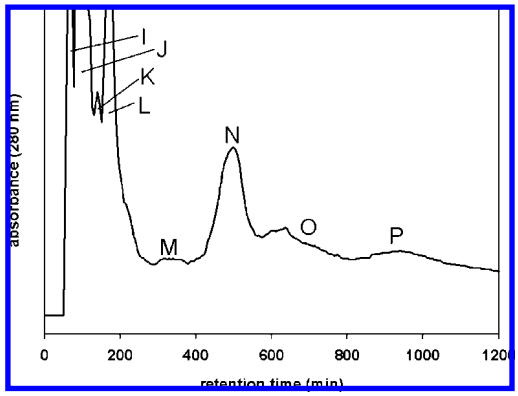

Figure 7. Separation of diethyl ether extract from rooibos tea by MLCCC: I–K, Mixture of flavonoids; L, gallic acid (**15**); M, gentisic acid (**18**); N, protocatechuic acid (**16**); O, syringic acid (**23**); P, vanillic acid (**21**) and caffeic acid (**22**).

= 20.5 min) *m/z* 308 ($M^{+\bullet}$, 2× silylated, 24%), 293 (53%), 249 (22%), 219 (35%), 179 (10%), 147 (15%), and 73 (100%); salicylic acid (**25**; RT = 11.8 min) *m/z* 267 ($M^{+\bullet}$, 2× silylated, 100%), 193 (7%), 149 (10%), 135 (12%), 91 (7%), and 73 (68%); ferulic acid (**26**; RT = 23.2 min) *m/z* 338 ($M^{+\bullet}$, 2× silylated, 38%), 323 (32%), 308 (27%), 293 (16%), 249 (19%), 219 (14%), 147 (26%), 117 (13%), and 73 (100%); sinapinic acid (**27**; RT = 25.2 min) *m/z* 368 ($M^{+\bullet}$, 2× silylated, 25%), 353 (23%), 338 (30%), 323 (11%), 129 (15%), 117 (26%), 73 (100%).

Data from *p*-coumaric acid (**24**) and ferulic acid (**26**) correspond to Lin et al. (*18*).

The residual stationary phase contained nonpolar aglycons such as (+)-catechin (**20**), quercetin (**28**), luteolin (**29**), and chrysoeriol (**30**) (**Figure 9**). For isolation of **29** + **30** the solventless residuum was separated by preparative thin-layer chromatography. After elution, target material was derivatized and injected into the HRGC-MS system (temperature program 2). The following polyphenolic structures were unequivocally identified by comparison with authentic material: chrysoeriol (**30**; RT = 18.5 min) *m/z* 486 ($M^+ - 15$, 5× silylated, 1%), 371 (69%), 313 (7%), 281 (10%), 239 (28%), 207 (29%), 203 (35%), 147 (85%), 129 (51%), 117 (37%), 103 (27%), 75

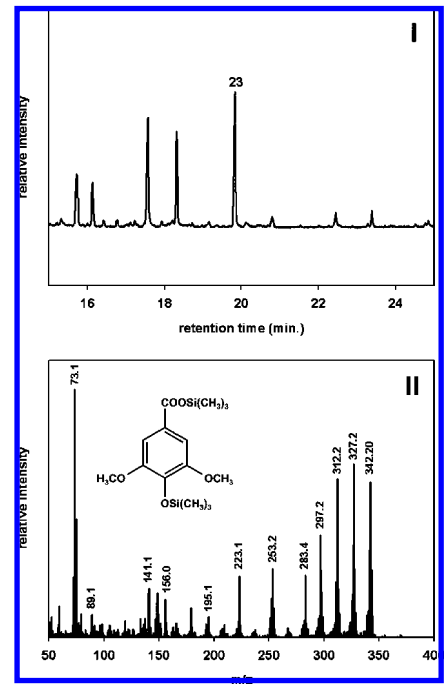

Figure 8. Signal O (**Figure 4**) of MLCCC separation of diethyl ether extract was derivatized by silylation: (I) HRGC-MS chromatogram, syringic acid (**23**) eluted at 19.8 min; (II) corresponding EI-mass spectrum.

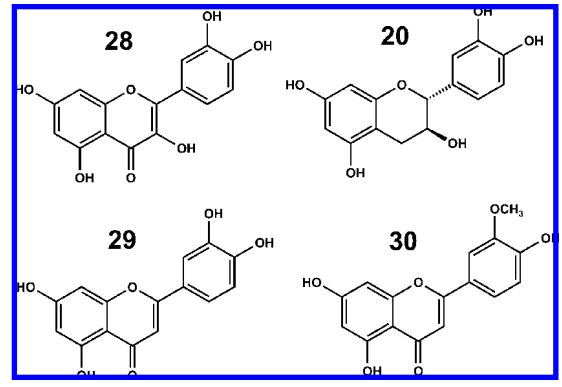

Figure 9. Aglycons isolated from the stationary phase of diethyl ether extract after MLCCC separation: **28**, quercetin; **20**, (+)-catechin; **29**, luteolin; **30**, chrysoeriol.

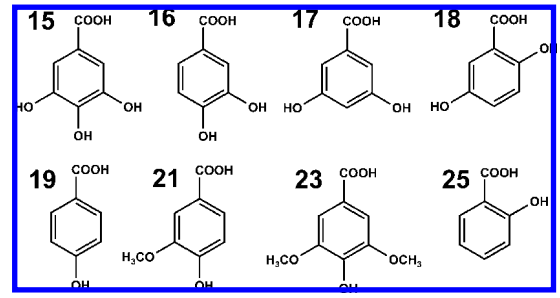

Figure 10. Hydroxybenzoic acids isolated from diethyl ether extract: **15**, gallic acid; **16**, protocatechuic acid; **17**, 3,5-dihydroxybenzoic acid; **18**, gentisic acid; **19**, *p*-hydroxybenzoic acid; **21**, vanillic acid; **23**, syringic acid; **25**, salicylic acid.

(100%), and 73 (96); luteolin (**29**; RT = 23.7 min) *m/z* 574 ($M^{+\bullet}$, 4× silylated, 1%), 488 (2%), 429 (2%), 399 (27%), 281 (10%), 207 (38%), 147 (77%), 129 (30%), 75 (100%), and 73 (62%). Quercetin (**28**) and (+)-catechin (**20**) could be unambiguously identified direct from the stationary phase by HRGC-MS (temperature program 2) after silylation: quercetin (**30**; RT

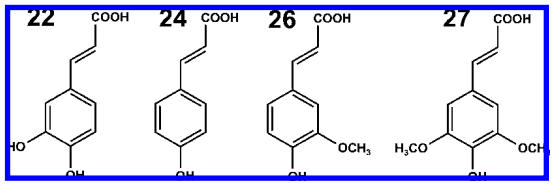

Figure 11. Hydroxycinnamic acids isolated from diethyl ether extract: **22**, caffeic acid; **24**, *p*-coumaric acid; **26**, ferulic acid; **27**, sinapinic acid.

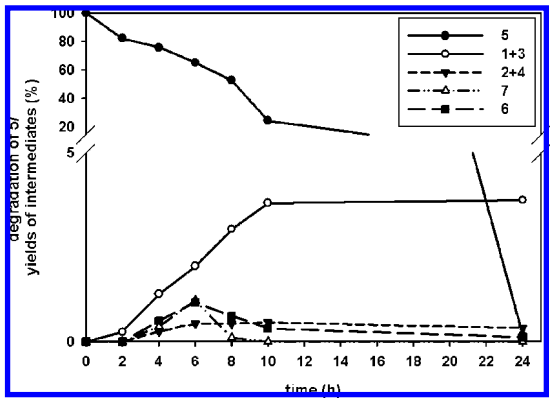

Figure 12. Degradation of aspalathin **5** to (*R*)/(*S*)-eriodictyol-6-*C*-*β*-D-glucopyranoside (**1** + **3**), (*R*)/(*S*)-eriodictyol-8-*C*-*β*-D-glucopyranoside (**2** + **4**), orientin (**6**), and isoorientin (**7**). Yields of intermediates are calculated on the basis of the initial concentration of aspalathin.

= 34.7 min) *m*/*z* 486 ($M^+ - 15$, 5× silylated, 1%), 371 (69%), 313 (7%), 281 (10%), 239 (28%), 207 (29%), 203 (35%), 147 (85%), 129 (51%), 117 (37%), 103 (27%), 75 (100%), and 73 (96); (+)-catechin (**20**; RT = 26.40 min) *m*/*z* 650 ($M^{+\bullet}$, 5× silylated, 7%), 578 (8%), 488 (3%), 383 (16%), 368 (100%), 296 (70%), 280 (66%), 179 (44%), 73 (89%), and 75 (10%). Data were in line with Ferreira et al. (*8*), Fischer et al. (*19*), and Amani et al. (*20*).

In conclusion the following substances from *A. linearis* were isolated and identified: (*S*)/(*R*)-eriodictyol-6-*C*-*β*-D-glucopyranoside (**1** + **3**), (*S*)/(*R*)-eriodictyol-8-*C*-*β*-D-glucopyranoside (**2** + **4**), aspalathin (**5**), orientin (**6**), isoorientin (**7**), vitexin (**8**), nothofagin (**9**), isovitexin (**10**), rutin (**11**), hyperoside (**12**), isoquercitrin (**13**), chlorogenic acid (5-CQA, **14**), gallic acid (**15**), protocatechuic acid (**16**), 3,5-dihydroxybenzoic acid (**17**), gentisic acid (**18**), *p*-hydroxybenzoic acid (**19**), (+)-catechin (**20**), vanillic acid (**21**), caffeic acid (**22**), syringic acid (**23**), *p*-coumaric acid (**24**), salicylic acid (**25**), ferulic acid (**26**), sinapinic acid (**27**), quercetin (**28**), luteolin (**29**), and chrysoeriol (**30**). Within this context **2** + **4**, **12**, **14**, **15**, **17**, **18**, **25**, and **27** were isolated from rooibos for the first time. Identified benzoic and cinnamic acids are shown in **Figure 10** and **Figure 11**. The established method is able to isolate multiple and minor polyphenolic substances and applicable to further natural products.

Degradation of Dihydrochalcones. Prolonged incubation of flavanone-*C*-glycosides resulted in several distinct structures.

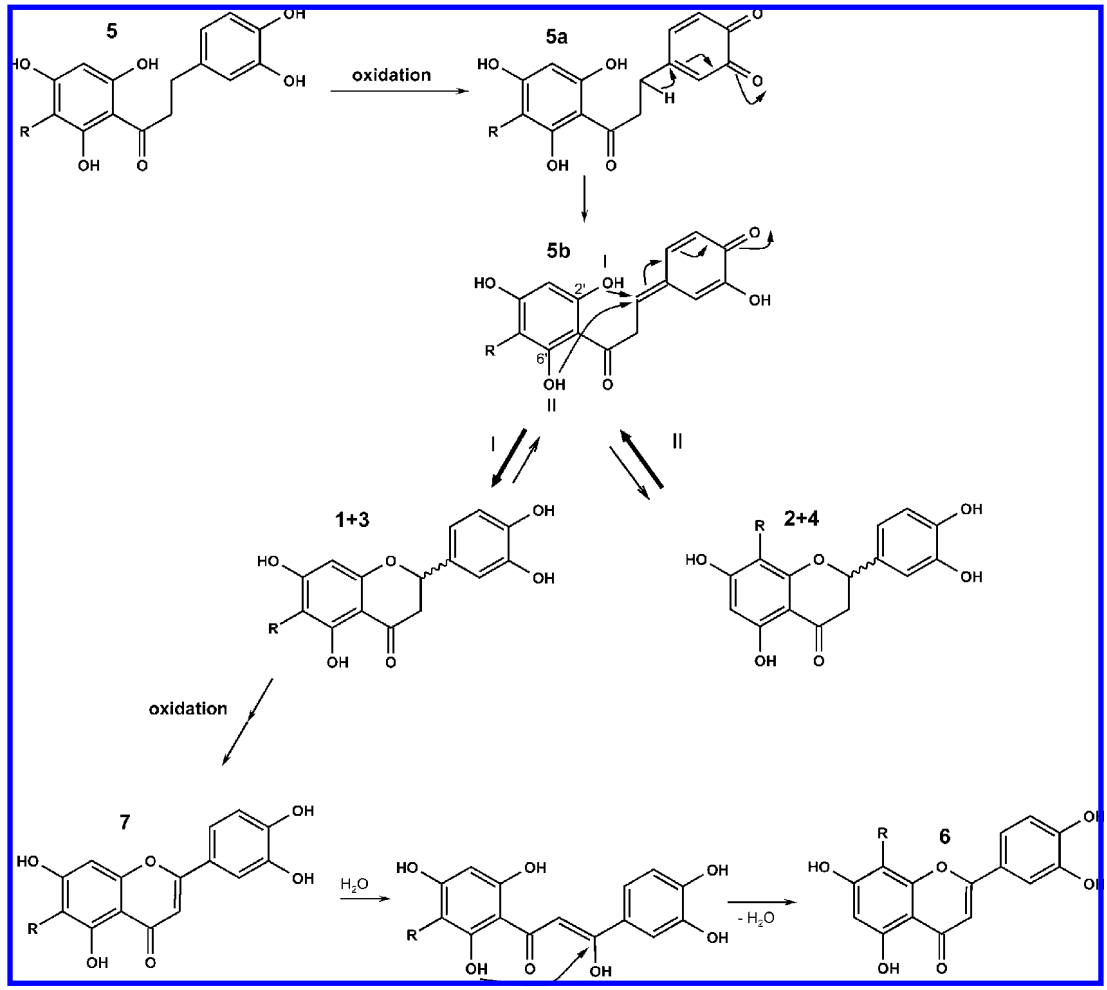

Figure 13. Oxidative degradation of aspalathin (**5**) to orientin (**6**) and isoorientin (**7**). Eriodictyols **1–4** (1-(*S*)-eriodictyol-6-*C*-*β*-D-glucopyranoside, 2-(*S*)-eriodictyol-8-*C*-*β*-D-glucopyranoside, 3-(*R*)-eriodictyol-6-*C*-*β*-D-glucopyranoside, 4-(*R*)-eriodictyol-6-*C*-*β*-D-glucopyranoside) are key intermediates. R = glucose.

Thus, the mechanisms of **5** degradation were studied in-depth. Compound **5** was incubated in phosphate buffer for 48 h (**Figure 12**). The half-life of **5** was calculated as 8 h. After 48 h, all structures were degraded to high molecular uncharacterized material and no discrete signals were detectable in HPLC-DAD. During the process eriodictyols **1** + **3** were the major products coinciding with minor concentrations of **2** + **4** in a stable ratio. Compounds **6** and **7** were also found with a maximum at 6 h. In contrast to a relative slow degradation of **6**, **7** was no longer detectable after 10 h.

The degradation of **5** to eriodictyols **1**–**4** must be explained by oxidation via *o*-quinone (**5a**; **Figure 13**). This structure then rearranges to quinine methide (**5b**), which allows fast conversion of isolated single eriodictyols into a stable equilibrium. Reaction step from **5b** to **1** + **3** was reversible, because incubations of (*S*)-eriodictyol-6-*C*-*β*-D-glucopyranoside immediately changed to a 1:1 mixture of **1** + **3** (**Figure 3**) and, more slowly and to a much lower extent, to the eriodictyol-8-*C*-*β*-D-glucopyranosides **2** + **4**. In equilibrium the ratio of **1** + **3** to **2** + **4** was about 10 to 1. Reactions of authentic **4** yielded **1** + **3**, while **4** was readily decomposed. Reactions of **1** + **3** also produced **7** and, unexpectedly, even higher amounts of **6**. In contrast, **2** + **4** never resulted in any **6**. This excludes direct oxidation of **2** + **4** to **6**. Compounds **6** and **7** were also incubated separately. Isoorientin was converted to orientin, although it was only a minor product among uncharacterized brown material. This is an irreversible reaction step, because **6** was not converted to **7**. Conversion must be initiated by opening of the vinyl ester structure of **7** followed by bond rotation and recyclization, also known as Wessely−Moser rearrangement. Conversion including reductive steps could be excluded as no eriodictyols were formed. During separate incubations of isolated **6** and **7**, degradation of **7** (half-life, 135 h) to brown products was considerably faster than degradation of **6** (half-life, 208 h). This also undermines the notion that degradation from **2** + **4** to **6** was not detectable because of a relative instability of **6**. The understanding of these complex reaction mechanisms is prerequisite to gain further insights into the chemical pathways during the fermentation process of rooibos.

ACKNOWLEDGMENT

We thank D. Ströhl from the Institute of Organic Chemistry, Halle, Germany, for recording NMR spectra, and J. Schmidt from the Leibnitz Institute of Plant Biochemistry, Halle, Germany, for performing LC-MS/accurate mass analysis.

LITERATURE CITED

(1) Erickson, L. Rooibos tea: Research in antioxidant and antimutagenic properties. *HerbalGram* **2003**, *59*, 34–45.
(2) Morton, J. F. Rooibos tea, Aspalathus linearis, a caffeineless, low tannine beverage. *Econ. Bot.* **1983**, *37*, 164–173.
(3) Koeppen, B. H.; Smith, J. B.; Roux, D. G. The flavone *C*-glycosides and flavonol *O*-glycosides of Aspalathus accuminatus (rooibos tea). *Biochem. J.* **1962**, *83*, 507–511.
(4) Koeppen, B. H. *C*-Glycosylflavonoids—The chemistry of orientin and isoorientin. *Biochem. J.* **1965**, *97*, 444–448.
(5) Koeppen, B. H.; Roux, D. G. Aspalathin, a novel *C*-glycosylflavonoid from Aspalathus linearis. *Tetrahedron Lett.* **1965**, *39*, 3497–3503.
(6) Snyckers, F. O.; Salemi, G. Studies of the South African medicinal plants (isolation and identification of Qquercetin and luteolin). *J. S. Afr. Chem. Inst.* **1974**, *27*, 5–7.
(7) Rabe, C.; Steenkamp, J. A.; Joubert, E. Phenolic metabolites from rooibos tea (Asphalatus linearis). *Phytochemistry* **1994**, *35*, 1559–1565.
(8) Ferreira, D.; Marais, C.; Steenkamp, J. A.; Joubert, E. Rooibos Tea a Likely Health Food Supplement. *Proceedings of Recent Developments of Technologies on Fundamental Foods for Health*; Korean Society of Food Science and Technology: Seoul, Korea, 1995, pp73–88.
(9) Marais, C.; van Rensberg, W. J.; Ferreira, D.; Steenkamp, J. A. (S)- and (R)-Eriodictyol-6-C-*β*-D-glucopyranoside, novel keys to the fermentation of rooibos (Aspalathus linearis). *Phytochemistry* **2000**, *55*, 43–49.
(10) Joubert, E. HPLC quantification of the dihydrochalcones, aspalathin and Nnothofagin in rooibos tea (Aspalathus linearis) as affected by processing. *Food Chem.* **1996**, *55*, 403–411.
(11) Maillard, M.; Marston, A.; Hostettmann, K. High-Speed Countercurrent Chromatography of Natural Products. In *High-Speed Countercurrent Chromatography*, 1st ed.; Ito, Y.; Conway, W. D.; Wiley: New York, 1996; Vol. 132.
(12) Koeppen, B. H.; Roux, D. G. C-Glycosylflavonoids. The chemistry of aspalathin. *Biochem. J.* **1966**, *99*, 604–609.
(13) Bramati, L.; Minoggio, M.; Gardana, C.; Simonetti, P.; Mauri, P.; Pietta, P. Quantitative characterization of flavonoid compounds in rooibos tea (*Aspalathus linearis*) by LC-UV/DAD. *J. Agric. Food Chem.* **2002**, *50*, 5513–5519.
(14) Hillis, W. E.; Inoue, T. The polyphenols of nothofagus species-II. The heartwood of Nothofagus fusca. *Phytochemistry* **1967**, *6*, 59–67.
(15) Philbin, C. S.; Schwartz, S. J. Resolution of diastereomeric flavonoid (1S)-(−)-camphanic acid esters via reversed-phase HPLC. *Phytochemistry* **2007**, *68*, 1206–1211.
(16) Sawabe, A.; Nesumi, C.; Morita, M.; Matsumoto, S.; Matsubara, Y.; Komemushi, S. Glycosides in African dietary leaves, Hibiscus sabdariffa. *J. Oleo Sci.* **2005**, *54*, 185–191.
(17) Krasnov, E. A.; Raldugin, V. A.; Shilova, I. V.; Avdeeva, E. Yu. Phenolic compounds from Filipendula ulmaria. *Chem. Nat. Compd.* **2006**, *42*, 148–151.
(18) Lin, L. Z.; Harnly, J. M. A screening method for the identification of glycosylated flavonoids and other phenolic compounds using a standard analytical approach for all plant materials. *J. Agric. Food Chem.* **2007**, *55*, 1084–1096.
(19) Fischer, C. H.; Bischof, M.; Rabe, J. G. Identification of natural and early synthetic textile dyes with HPLC and UV/VIS-spectroscopy by diode array detection. *J. Liquid Chromatogr.* **1990**, *13*, 319–331.
(20) Amani, S. A.; Maitland, D. J.; Soliman, G. A. Hepatoprotective activity of Schouwia thebica webb. *Bioorg. Med. Chem. Lett.* **2006**, *16*, 4642–4628.
(21) Fossen, T.; Andersen, O. M. Spectroscopic techniques applied to flavonoids. In *Flavonoids—Chemistry, Biochemistry and Applications*, 1st ed.; Andersen, O. M., Markham K. R.; CRC Press, Taylor & Francis Group: Boca Rutan, Florida, 2006.
(22) Rayyan, S.; Fossen, T.; Nateland, H. S.; Andersen, O. M. Isolation and identification of flavonoids, including flavone rotamers, from the herbal drug 'Crataegi Folium Cum Flore' (Hawthorn). *Phytochem. Anal.* **2005**, *16*, 334–341.

Received for review December 19, 2007. Revised manuscript received February 22, 2008. Accepted February 24, 2008.

JF703701N